EUR 201.e
REPRINT

EUROPEAN ATOMIC ENERGY COMMUNITY — EURATOM

DISLOCATIONS AND WIDE STACKING FAULTS IN WURTZITE TYPE CRYSTALS : ZINC SULFIDE AND ALUMINIUM NITRIDE

by

S. AMELINCKS (C.E.N.), H. BLANK (EURATOM)
P. DELAVIGNETTE (C.E.N.)

1963

Euratom - United States Agreement for Cooperation
Work done by C.E.N.-Mol under the
Euratom contract No. 063 - 61 - 10 RDB

Reprinted from
Physica Status Solidi
No. 2 - 1962

EUR 201.e

REPRINT

DISLOCATIONS AND WIDE STACKING FAULTS IN WURTZITE TYPE CRYSTALS - ZINC SULFATE AND ALUMINIUM NITRIDE by S. AMELINCKS (C.E.N.), H. BLANK (EURATOM), P. DELAVIGNETTE (C.E.N.).

Euratom-United States Agreement for Cooperation.
Work done by C.E.N.-Mol under the Euratom contract No. 063-61-10 RDB.
Reprinted from "Physica Status Solidi", No. 2-1962, pages 1660-1669.

Vapour grown ZnS and AIN crystals of wurtzite structure are studied by transmission electron microscopy. The habit plane of the ZnS crystals is $< 11\bar{2}0 >$ and that of AIN (0001). The stacking fault energy is negative in hexagonal ZnS and positive in AIN at 20° C so that different patterns of dislocations and stacking faults are observed in the two wurtzite structures. In ZnS stacking faults in prism planes are found which show some uncommon properties.

EUR 201.e

REPRINT

DISLOCATIONS AND WIDE STACKING FAULTS IN WURTZITE TYPE CRYSTALS - ZINC SULFATE AND ALUMINIUM NITRIDE by S. AMELINCKS (C.E.N.), H. BLANK (EURATOM), P. DELAVIGNETTE (C.E.N.).

Euratom-United States Agreement for Cooperation.
Work done by C.E.N.-Mol under the Euratom contract No. 063-61-10 RDB.
Reprinted from "Physica Status Solidi", No. 2-1962, pages 1660-1669.

Vapour grown ZnS and AIN crystals of wurtzite structure are studied by transmission electron microscopy. The habit plane of the ZnS crystals is $< 11\bar{2}0 >$ and that of AIN (0001). The stacking fault energy is negative in hexagonal ZnS and positive in AIN at 20° C so that different patterns of dislocations and stacking faults are observed in the two wurtzite structures. In ZnS stacking faults in prism planes are found which show some uncommon properties.

EUR 201.e

REPRINT

DISLOCATIONS AND WIDE STACKING FAULTS IN WURTZITE TYPE CRYSTALS - ZINC SULFATE AND ALUMINIUM NITRIDE by S. AMELINCKS (C.E.N.), H. BLANK (EURATOM), P. DELAVIGNETTE (C.E.N.).

Euratom-United States Agreement for Cooperation.
Work done by C.E.N.-Mol under the Euratom contract No. 063-61-10 RDB.
Reprinted from "Physica Status Solidi", No. 2-1962, pages 1660-1669.

Vapour grown ZnS and AIN crystals of wurtzite structure are studied by transmission electron microscopy. The habit plane of the ZnS crystals is $< 11\bar{2}0 >$ and that of AIN (0001). The stacking fault energy is negative in hexagonal ZnS and positive in AIN at 20° C so that different patterns of dislocations and stacking faults are observed in the two wurtzite structures. In ZnS stacking faults in prism planes are found which show some uncommon properties.

phys. stat. sol. 2, 1660 (1962)

Departement Fysika Vaste Stof, Studiecentrum voor Kernenergie, Mol

Dislocations and Wide Stacking Faults in Wurtzite Type Crystals: Zinc Sulfide and Aluminium Nitride

By

H. BLANK[1]) P. DELAVIGNETTE, and S. AMELINCKX

Vapour grown ZnS and AlN crystals of wurtzite structure are studied by transmission electron microscopy. The habit plane of the ZnS crystals is $\langle 11\bar{2}0\rangle$ and that of AlN (0001). The stacking fault energy is negative in hexagonal ZnS and positive in AlN at 20 °C so that different patterns of dislocations and stacking faults are observed in the two wurtzite structures. In ZnS stacking faults in prism planes are found which show some uncommon properties.

Aus der Dampfphase gezüchtete ZnS- und AlN-Kristalle mit Wurtzitstruktur sind elektronenmikroskopisch untersucht worden. Die Habitusfläche der ZnS-Kristalle ist $\langle 11\bar{2}0\rangle$ und die der AlN-Kristalle (0001). Hexagonales ZnS hat bei 20 °C eine negative Stapelfehlerenergie, während AlN eine positive Stapelfehlerenergie besitzt. Deshalb wurden verschiedene Dislokations- und Stapelfehlerkonfigurationen in den beiden Wurtzitstrukturen festgestellt. In ZnS wurden Stapelfehler in Prismenflächen gefunden, die einige ungewöhnliche Eigenschaften zeigen.

Observations of dislocations in ZnS have been limited so far to etch pit studies [1, 2]. The presence of stacking faults, of polytypes and of stacking disorder was deduced by means of x-ray diffraction [3]. Birefringence bands in vapour grown crystals have been attributed to stacking faults and to lamella of wurtzite in a sphalerite matrix [4]. In view of the importance of ZnS as a luminescent material and also in view of a better understanding of the origin of the enormous photovoltages produced on illumination in ZnS whiskers [5] it is of interest to know more about the fault structure. It is believed that stacking disorder plays a role in these phenomena [6].

In this note some preliminary results of an electron microscopic study of vapour grown ZnS platelets are presented. The crystals were grown in flowing argon, the ZnS powder charge being held at a temperature of about 1200 °C. The vapour was allowed to condense on the outside of the end of a closed quartz tube cooled from the inside by an air stream. Under these conditions the crystals are growing in the wurtzite structure as small flat needles with habit plane $\langle 11\bar{2}0\rangle$. The wurtzite structure is represented in projection on the basal plane and in cross section parallel to the $\langle 1\bar{1}00\rangle$ plane in Fig. 1. Wurtzite is known as the high temperature modification of ZnS but the crystals do not transform into sphalerite on cooling through the transformation temperature at 1020 °C.

The as grown crystals seem to contain very few b-faults (stacking faults in basal planes). Under prolonged electron bombardment half dislocations could quite often be seen moving across the crystals. The nucleation of these partials seems always to take place at cracks, inclusions or other very big irregularities

[1]) Permenant address: EURATOM, Brussels (Belgium).

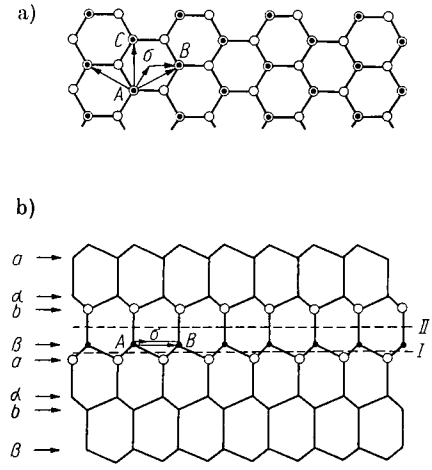

Fig. 1. Schematic view of the wurtzite structure.
a) Projection on the basal plane, the possible shear vectors of partial dislocations in the basal plane are indicated by $A\sigma$, $B\sigma$, $C\sigma$ and their negatives.
b) Side view of the wurtzite structure along the AC direction, $\langle 1\bar{1}00\rangle$ type plane. The two possible glide planes are indicated by I and II. Glide planes of type II can only contain perfect dislocations

in the crystals. From visual inspection the movement of the partials was in most cases rather steady and the speed of the order of 10^3 to 10^4 Å/sec. Several cases have been observed where half dislocations had stopped in the foil, but normally they moved right through the crystal and disappeared at the edges. Heating the foil with the electron beam resulted locally in partial evaporation of the foil and in the production of more b-faults, but a complete transformation of the crystal into the cubic phase never occured. The movement of a single partial leaves behind a stacking fault and thus transforms a lamella of wurtzite into a

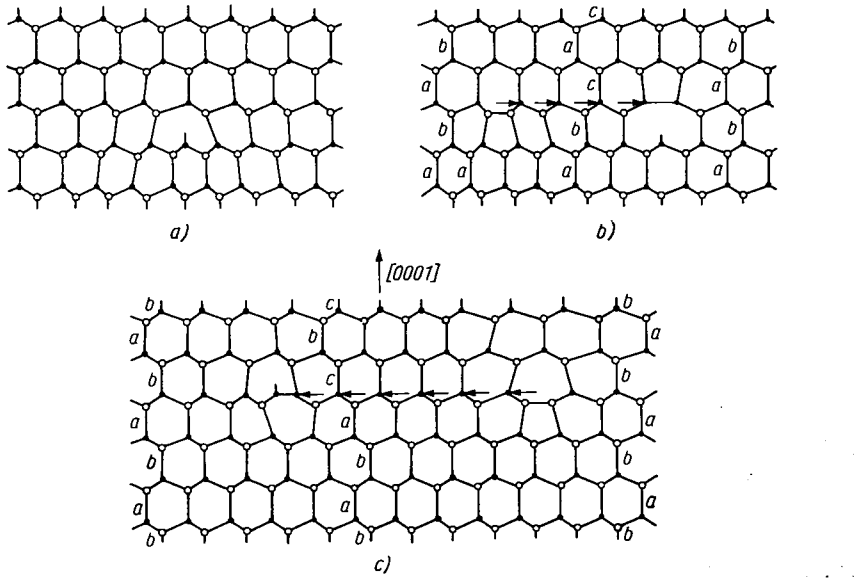

Fig. 2. Dislocations in the wurtzite structure, after ref. [7]
a) Undissociated dislocations with type II glide plane
b) Dislocation of Fig. 2a dissociated into partials with formation of a fault $b\,\beta\,a\,\alpha\,b\,\beta\,c\,\gamma\,a\,\alpha\,c\,\gamma\,a\,\alpha\ldots$ The dissociation has taken place in the next type I glide plane *above* the glide plane of the perfect dislocation!
c) The dislocation of Fig. 2a, dissociated into partials in the next type I glide plane *below* the type II glide plane of the entire dislocation. A fault $b\,\beta\,a\,\alpha\,b\,\beta\,a\,\alpha\,c\,\gamma\,b\,\beta\,c\,\gamma\,b\,\beta$ is formed

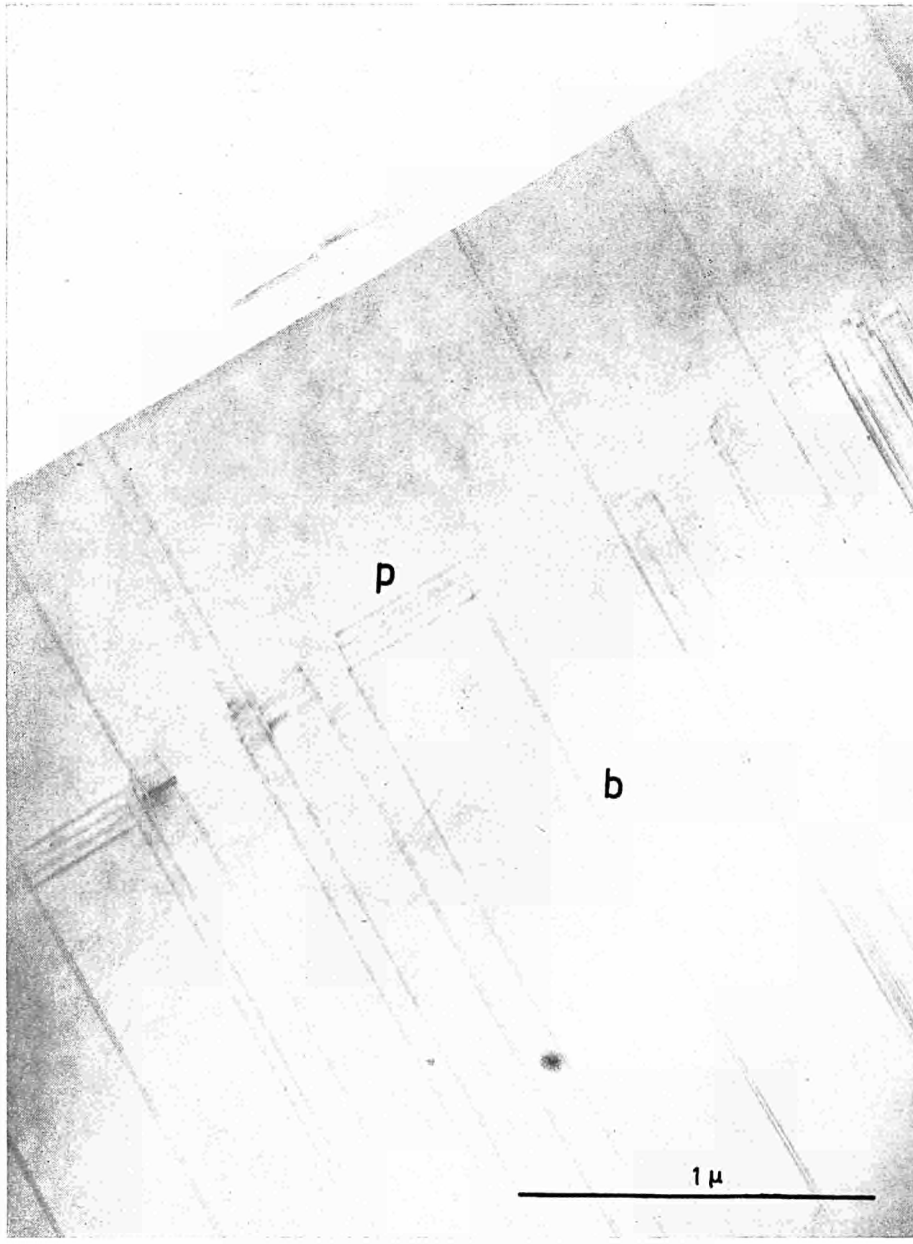

Fig. 3. Crystal foil of ZnS containing two types of stacking faults. The faults denoted by b are lying in basal planes and those denoted by p are lying in prism planes

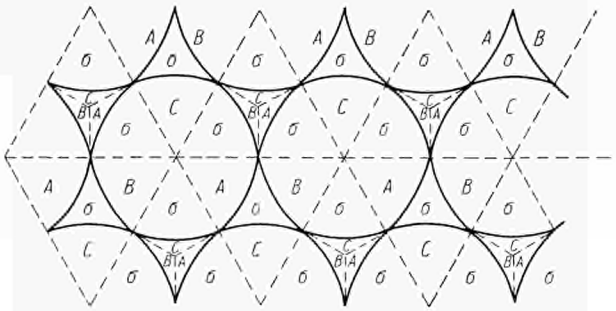

Fig. 4. Schematic drawing of a pattern of extended nodes expected to arise by interaction of two sets of dislocations of the types shown in Fig. 2

lamella of sphalerite. From these observations one can conclude that the stacking fault energy in hexagonal ZnS at room temperature is effectively negative, i. e. dislocations in basal planes split at once in infinitely wide ribbons. However, in thin crystals the nucleation of these dislocations is obviously difficult and only possible at very coarse crystal defects.

The model of a complete dislocation in a basal plane and the way how it is expected to split into partials is shown in Fig. 2a, 2b, and 2c respectively. The shear vector of a partial is denoted by $A\,\sigma$, $\sigma\,A$, $B\,\sigma$, . . . etc. in Fig. 1. Such isolated partials and the associated wide stacking faults are visible in Fig. 3. There the b-faults show up only as narrow dark lines because the electron beam is almost parallel to the basal planes in the normal orientation of the crystals, $\langle 11\bar{2}0\rangle$ being the plane of the foils. The faults described here are those inferred from x-ray diffraction studies. The dissociation of a given perfect dislocation, see Fig. 2a, into partials can take place in two different ways depending on the glide planes in which it occurs. In Fig. 2b it took place in the type I glide plane *above* the type II glide plane of the perfect dislocation and in Fig. 2c the dissociation has

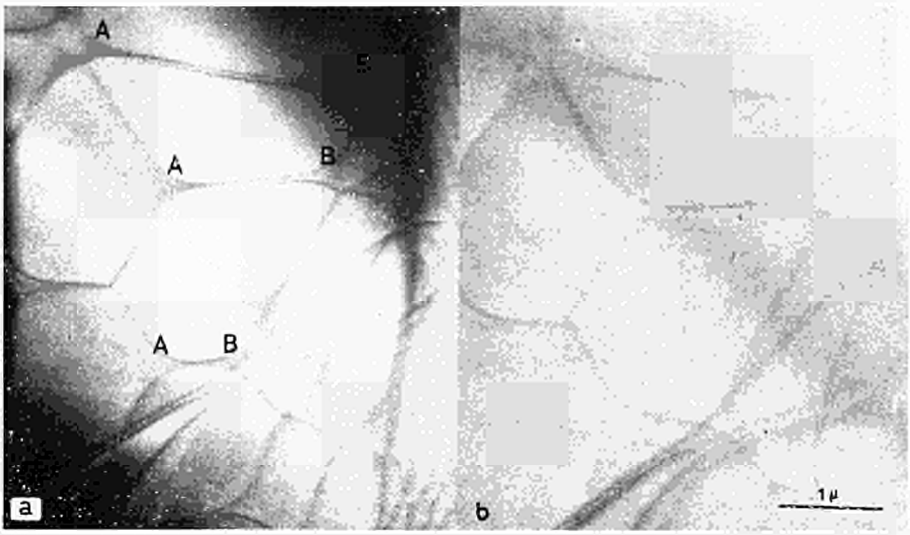

Fig. 5. Examples of neighbouring extended nodes according to Fig. 4 found in AlN. This has the same structure but higher (positive) stacking fault energy than hexagonal ZnS. a) and b) show the same area with different partials out of contrast. This allows to recognize the three families of partials with common Burgers vectors. In particular one can see easily the crossing over of the partials between A and B

occured in the type I glide plane *below* the type II glide plane of the perfect dislocation. The first case gives rise to a stacking fault

$$b\,\beta\,a\,\alpha\,b\,\beta\,c\,\gamma\,a\,\alpha\,c\,\gamma\,a\,\alpha\,\ldots$$

whereas the second dissociation results in a fault

$$b\,\beta\,a\,\alpha\,b\,\beta\,a\,\alpha\,c\,\gamma\,b\,\beta\,c\,\gamma\,b\,\beta\,\ldots$$

Both types of faults have the same energy and are therefore equally probable. If two sets of dislocations produce a cross-grid in a basal plane a hexagonal network is formed with all nodes extended as shown in Fig. 4. This has in fact been

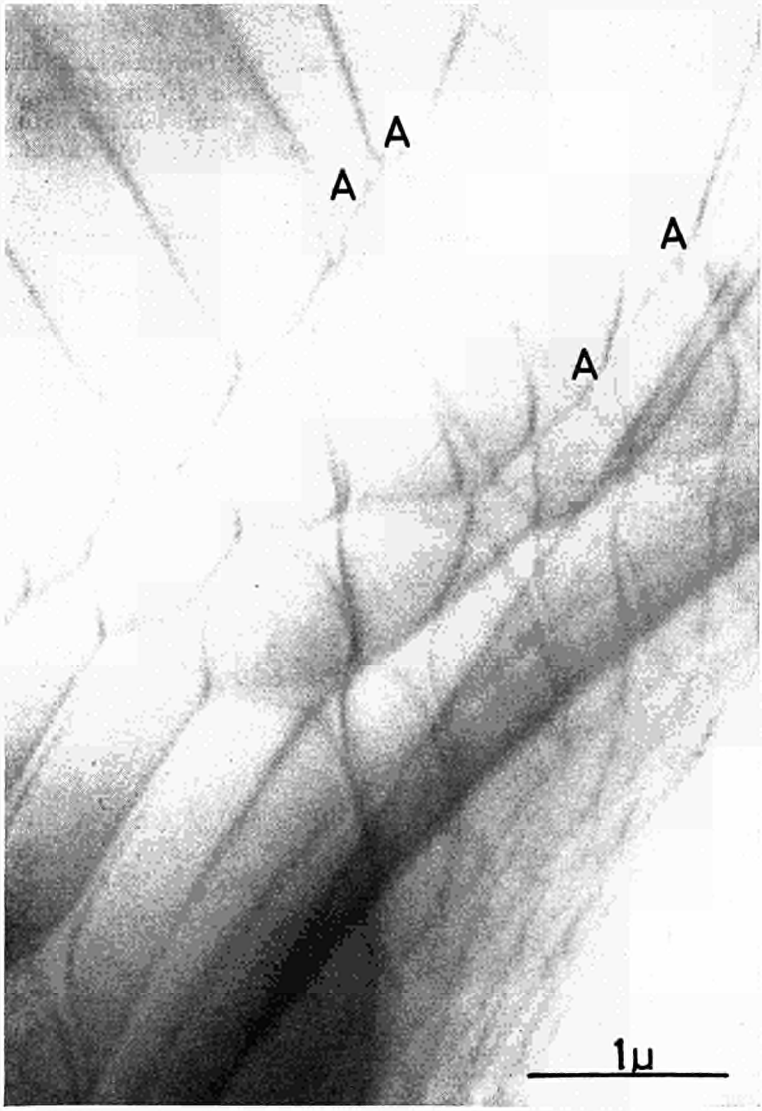

Fig. 6. Pattern of another type of nodes in AlN. The same type has been observed in graphite (ref. [8]). Segments of double ribbons are visible at A

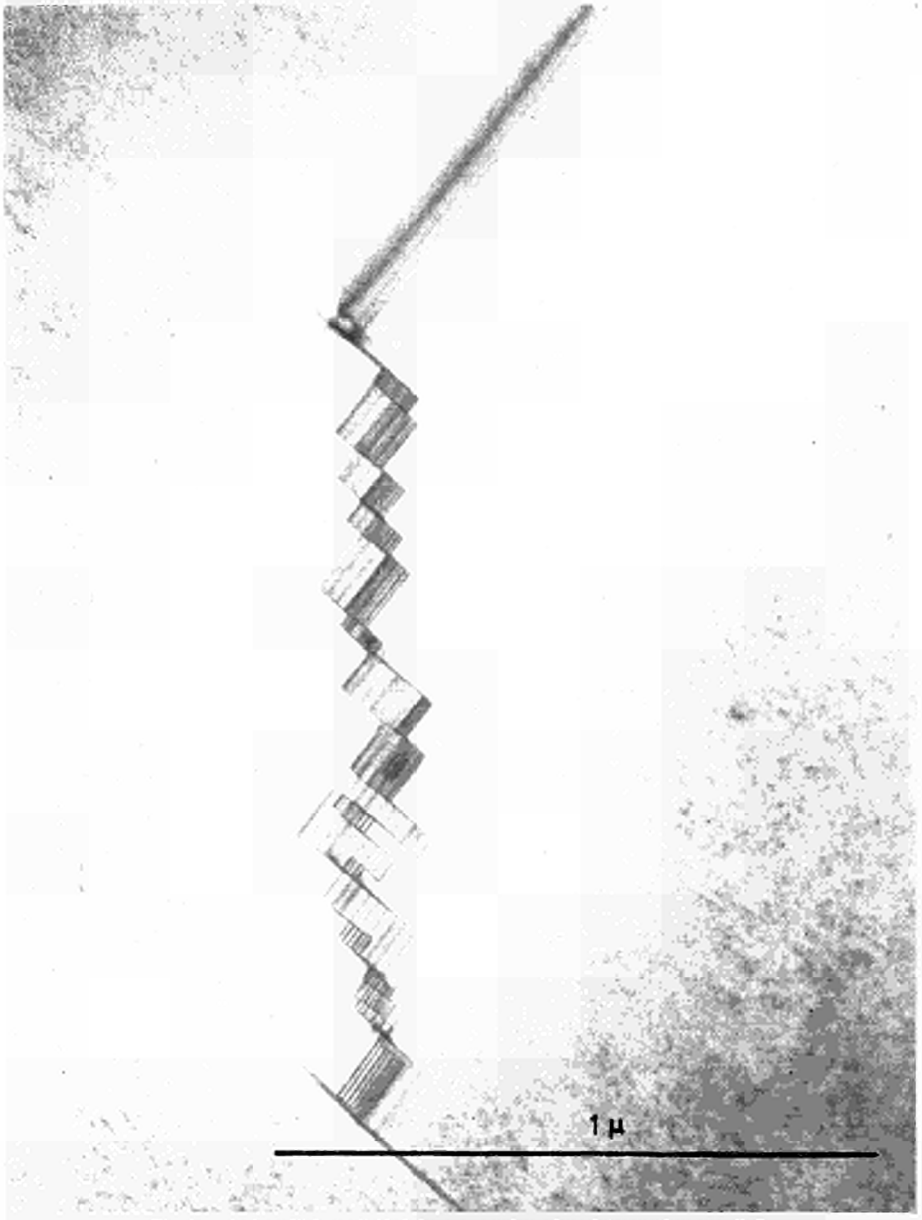

Fig. 7. p-faults which are folded from one prism plane into another one, ZnS

observed in AlN crystal foils of habit plane ⟨0001⟩. In Fig. 5 one can see at *A* and *B* two neighbouring extended nodes of the type schematically drawn in Fig. 4. A different pattern of nodes in AlN which is of the same type as those observed in graphite [8] is given in Fig. 6. The nodes result from the intersection of two stacking fault ribbons lying in adjacent *c*-planes. They are characterized by a small segment of double ribbon, indicated by *A* in Fig. 6. In the ZnS

Fig. 8. Schematic drawing of the junctions found between b- and folded p-faults in ZnS

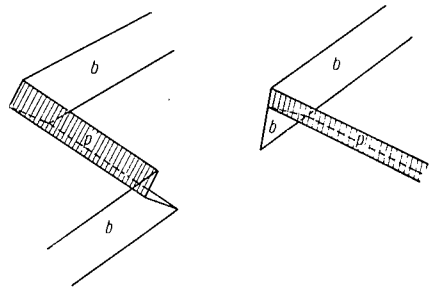

crystals used here such a pattern cannot be observed as a consequence of the orientation of the basal planes. A difficulty for the development of such a pattern in ZnS may perhaps be its negative stacking fault energy.

Besides the faults in the basal planes rather unexpectedly other faults were found in prism planes (p-faults) of ZnS. Some of these are also visible in Fig. 3. The fault plane is presumably of the type $\langle 4\bar{3}\bar{1}0\rangle$. The exact indices are still somewhat in doubt. These p-faults are always connected with b-faults forming an arrangement at right angles, Fig. 3. Often the p-faults do not ly completely in one plane but change sharply into another prism plane intersecting the first one in a line parallel to the c-axis. Examples of such folded p-faults are shown in Fig. 7. Fig. 8 represents schematically the three types of connections between b- and folded p-faults, which have been found hitherto. The p-faults show still another special feature. If the crystal is of such an orientation that the p-fault itself is out of contrast, in the area of the fault other details appear in contrast. These details may have very different aspects as can be seen from Fig. 9 and 10. Also closed loops composed of both types of stacking faults have been found, see Fig. 11. In this connection it is important that the junction between a p- and a b-fault may or may not contain a dislocation as is indicated in Fig. 10 by the arrows.

A more detailed account will be published elsewhere.

Acknowledgements

We wish to thank Prof. Dr. M. D' HONT, scientific director of S.C.K., and EURATOM (Brussels) for permission to publish this paper. Thanks are due to Dr. DIEMER of the Philips Laboratories (Eindhoven, Netherlands) for providing us with some specimens on which the early observations were made. Thanks are also due to Mr. J. NICASY for skilful preparation of specimens and to Mr. H. BEYENS for his careful photographic work.

References

[1] W. DEKEYSER, S. AMELINCKX, E. VOTAVA, and G. VANDERMEERSCHE, Phil. Mag. **44**, 1142 (1953).
[2] H. HARTMANN, phys. stat. sol. **2**, 929 (1962).
[3] H. JAGODZINSKI, Acta cryst. **2**, 201, 208, 298 (1949).
[4] H. SAMELSON, J. appl. Phys. **32**, 309 (1961).
[5] W. J. MERZ, Helv. phys. Acta **31**, 625 (1958).
[6] G. F. NEUMARK, Phys. Rev. **125**, 838 (1962).
[7] P. DELAVIGNETTE, H. B. KIRKPATRICK, and S. AMELINCKX, J. appl. Phys. **32**, 1098 (1961).
[8] P. DELAVIGNETTE and S. AMELINCKX, J. Nucl. Mat. **5**, 16 (1962).

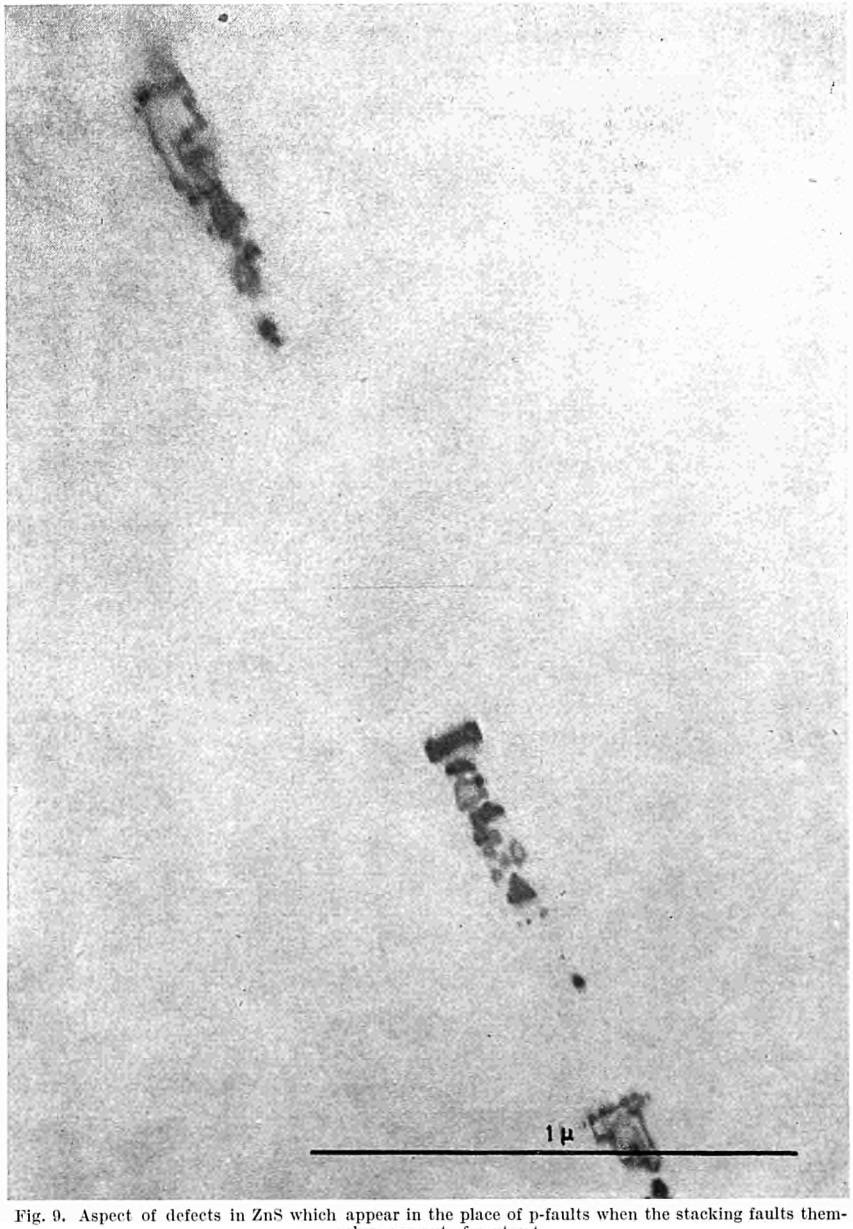

Fig. 9. Aspect of defects in ZnS which appear in the place of p-faults when the stacking faults themselves are out of contrast

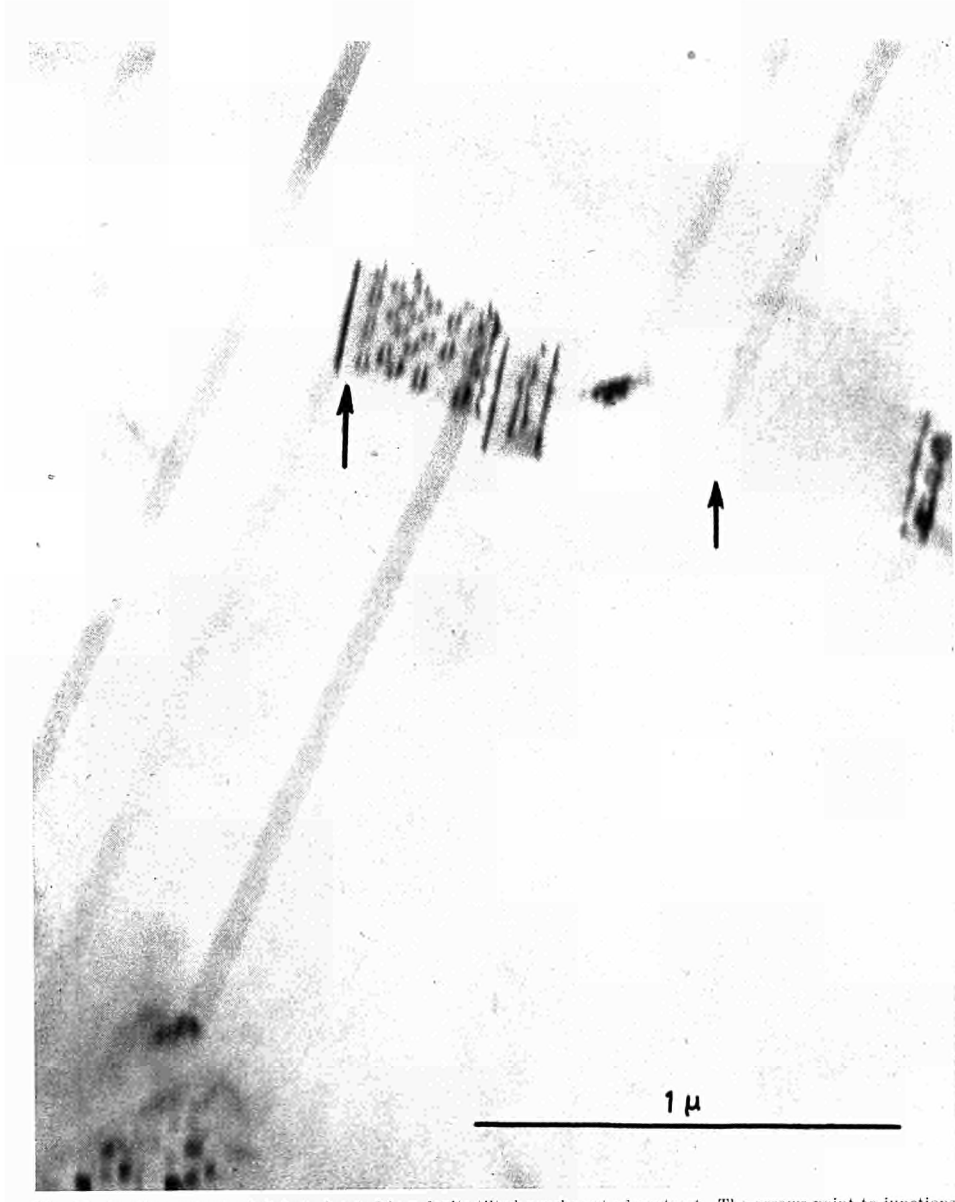

Fig. 10. Another aspect of defects located in p-faults tilted nearly out of contrast. The arrows point to junctions between b- and p-faults with and without a dislocation

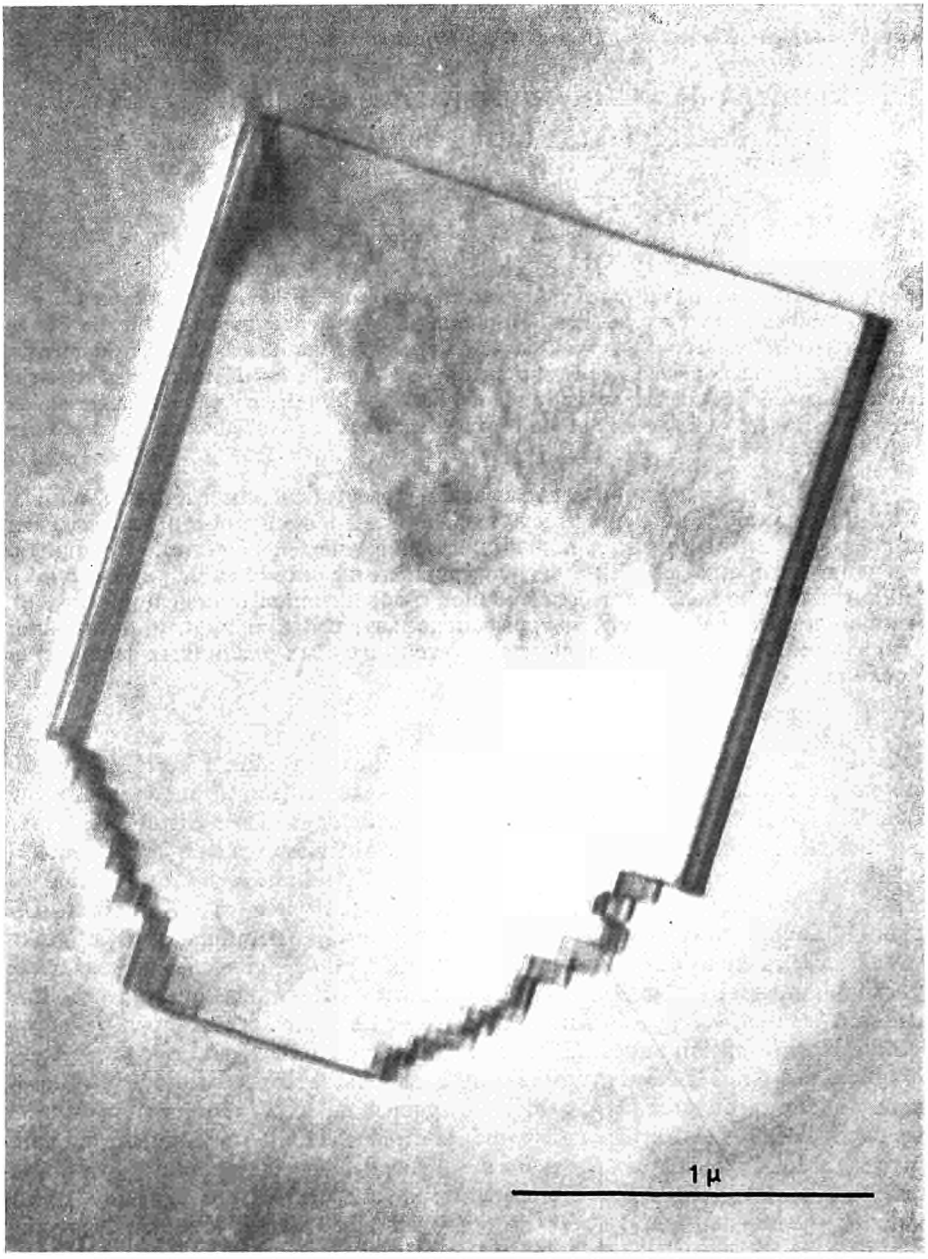

Fig. 11. Closed loop of stacking faults which is composed of alternating b- and p-faults in ZnS

(Received September 14, 1962)

phys. stat. sol. 2, 1670 (1962)

Zentralinstitut für Kernphysik, Bereich Werkstoffe und Festkörper, Rossendorf bei Dresden

Bestimmung der Aktivierungsenergie für die Beweglichkeit von Gitterdefekten durch zeitlineares Aufheizen

Von
M. Balarin und A. Zetzsche

Es wird eine neue Methodik zur Auswertung experimenteller Ausheilkurven bei zeitlinearem Aufheizen und speziell zur Bestimmung der Aktivierungsenergie für die Beweglichkeit von Gitterstörungen vorgeschlagen. Dabei wird von den bekannten kinetischen Gleichungen für monomolekulare Reaktionen ausgegangen. Diese Methodik gestattet eine genauere und objektivere Auswertung als die bisher bei zeitlinearem Aufheizen angewandten Verfahren. Die Anwendbarkeit auf die verschiedenartigsten physikalischen Probleme wird demonstriert.

Предлагается новая методика для расшифровки экспериментальных кривых по отжигу при временно-линейном нагревании и в особенности для определения энергии активации для подвижности нарушений решетки. Исходными уравнениями являются кинетические уравнения мономолекулярных реакций. Данная методика позволяет более точное и обьективное определение по сравнению с другими методами, которые используются при временно-линейном нагревании. Применимость демонстрируется на самых различных физических проблемах.

Einleitung

Bei der Untersuchung der Ausheilung der durch Bestrahlung, Verformung oder eine andere Beanspruchung in Festkörpern erzeugten Gitterstörungen interessiert besonders die Aktivierungsenergie für die Beweglichkeit dieser Gitterdefekte. Es sind vielerlei Methoden zur Bestimmung dieser Aktivierungsenergie bekannt [1], am häufigsten werden isotherme und isochrone Verfahren angewandt. Eine besondere Art der Ausheiluntersuchungen erfolgt durch zeitlineares Aufheizen. Unabhängig davon, ob es sich bei der Wanderung und der Annihilation der Defekte um reine Elektronen- oder Ionenprozesse handelt, gilt die gleiche Kinetik für den Prozeßablauf. Bei einem Teil der Eigenschaften, die während der Ausheilung gemessen werden, erfolgt die Änderung mit der Zeit bzw. der Temperatur so,wie sich die Konzentration ändert (Fig. 1,a). In anderen Fällen wird der pro Zeiteinheit bzw. pro Grad Temperaturerhöhung ausheilende Konzentrationsanteil z. B. durch die freiwerdende Energie (Fig. 1,b) gemessen. Kurven dieser Art werden besonders häufig bei Lumineszenz- und Leitfähigkeitsuntersuchungen an Halbleitern erhalten, wo sich die Bezeichnung „Glow"-Kurven eingebürgert hat. Natürlich besteht zwischen den Konzentrations- und den „Energie"-Kurven eine eindeutige Beziehung. Zur Auswertung werden bei allen bisherigen Methoden nur besonders ausgezeichnete Einzelpunkte herangezogen, wie die Temperaturlage des Glow-Maximums u. a. oder es werden die empirischen experimentellen Kurven sogar ohne irgend eine numerische Auswertung angegeben. In dieser Hinsicht ist es sogar unverständlich, warum die Methoden zur Auswertung der Ausheilvorgänge so sehr unterschiedlich gehandhabt werden.

CDNA00201ENC